Cooperative oxygen ion dynamics in $Gd_2Ti_{2-y}Zr_yO_7$

K. J. Moreno, G. Mendoza-Suárez, and A. F. Fuentes
CINVESTAV-IPN Unidad Saltillo, Apdo. postal 663, 25000 Saltillo, Coahuila, Mexico

J. García-Barriocanal, C. León, and J. Santamaria
GFMC, Dpto. Física Aplicada III, Universidad Complutense Madrid, 28040 Madrid, Spain
(Received 16 February 2005; published 22 April 2005)

We report on dispersive conductivity measurements in the oxygen ion conductor $Gd_2(Ti_{2-y}Zr_y)O_7$. Increasing Zr content leads to higher concentration of oxygen vacancies and results in higher activation energies for long-range ion transport, whilst the microscopic energy barrier for single ion hopping remains constant. We find evidence that, besides oxygen binding energy, enhanced cooperativity in oxygen ion dynamics determines the activation energy for long-range diffusion.

DOI: 10.1103/PhysRevB.71.132301 PACS number(s): 66.30.−h

Oxygen ion conductors of fluorite structure, such as yttria stabilized zirconia (YSZ), are used commercially as electrolytes in solid oxide fuel cells.[1,2] Temperatures for applications of oxide conductors[3,4] are typically higher than 500 °C due to low conductivity values at lower temperatures. A major challenge is to increase oxygen conductivity to allow room temperature applications. Long-range migration of oxygen ions takes place by thermally activated hopping to adjacent oxygen vacancies, which yields a dc conductivity of the form $\sigma_{dc}=(\sigma_\infty/T)\exp(-E_{dc}/kT)$. Increasing conductivity, thus, would require increasing the prefactor σ_∞ and/or decreasing the activation energy E_{dc}. However, increasing the number of charge carriers to increase σ_∞ leads to an undesired increase in E_{dc} and eventually to lower conductivity values,[1] thus limiting the strategies to obtain high oxygen conductivity at lower temperatures. The origin of this behavior has remained not well understood.[1–4] Here we show that the increase of the activation energy E_{dc} is determined by cooperative effects in oxygen dynamics.

Among oxide-ion conductors, those of pyrochlore structure $A_2B_2O_7$ have been shown to be promising candidates to substitute materials currently used in fuel cells.[5–7] $Gd_2Ti_{2-y}Zr_yO_7$ pyrochlores are particularly interesting since the concentration of mobile oxygen vacancies can be increased by substitution of Zr for Ti, and oxygen ion conductivity shows the highest value found among materials with pyrochlore structure. For $y\approx 1.8$ the conductivity is comparable to that of YSZ (10^{-2} S/cm at 700 °C).[5] It has been recently suggested from molecular dynamics[8,9] and static lattice energy minimization simulations[10] that oxygen diffusion in $Gd_2Ti_{2-y}Zr_yO_7$ occurs by hopping from 48*f* to 48*f* sites. This result has been later confirmed by XPS measurements.[7] The oxygen occupancy of 48*f* sites is 1 (or very close to 1) for Zr contents below $y=0.6$, but decreases progressively as Zr content is further increased.[11] These vacancies in 48*f* sites are responsible for oxygen hopping and diffusion, and explain the increase of more than two orders of magnitude in dc conductivity at 600 °C observed when increasing Zr content from $Gd_2Ti_{1.4}Zr_{0.6}O_7$ to $Gd_2Zr_2O_7$.[5] On the other hand, the energy barrier for oxygen hopping from 48*f* to 48*f* sites has been previously calculated and shown to be much smaller than that observed in experimental conductivity data.[10,12] These facts make the series $Gd_2Ti_{2-y}Zr_yO_7$ an ideal system to investigate the possible existence of cooperative effects in the oxygen hopping dynamics and its influence in determining the activation energy of long-range ionic transport. Impedance spectroscopy is the appropriate technique to probe ion hopping dynamics[13] and will allow us to investigate this issue. Although electrical conductivity measurements of $Gd_2Ti_{2-y}Zr_yO_7$ have been reported in the past, previous works are only concerned with dc conductivity, and no analysis of the dispersion of the ac conductivity data has been made to gain information on the oxygen dynamics. We report here on impedance spectroscopy measurements of $Gd_2Ti_{2-y}Zr_yO_7$ at relatively low temperatures, where frequency dependence of the ac conductivity can be observed.

$Gd_2(Ti_{2-y}Zr_y)O_7$ samples with different Zr contents, $0\leqslant y\leqslant 2$, were prepared from the corresponding oxides. Cylindrical pellets 0.7 mm thick were prepared for electrical measurements, and sintered at 1500 °C. Silver electrodes (with diameter 7 mm) were painted at both faces. Impedance spectroscopy measurements were performed by using a LCR meter HP 4284A, in the frequency range 100 Hz–1 MHz, and varying temperature between 200 °C and 600 °C. All measurements were made under N_2 gas flow to ensure an inert atmosphere. Measurements were also done under air flow and no difference was observed.

Figure 1(a) shows the frequency dependence of the real part of the conductivity at several temperatures for a representative composition $Gd_2Ti_{0.2}Zr_{1.8}O_7$. At low temperature, a power law dependence is observed at high frequencies while conductivity is frequency independent at low frequencies. The decrease observed in conductivity values at low frequencies for the highest temperatures is due to blocking effects at grain boundaries. For the samples under study we distinguish bulk conductivity, grain boundary, and electrode blocking effects by measuring complex impedance at different temperatures. In Fig. 1 temperatures have been chosen to show bulk conductivity (the only pertinent to our analysis). The frequency dependence of bulk conductivity is well described by the so-called Jonscher empirical expression[14]

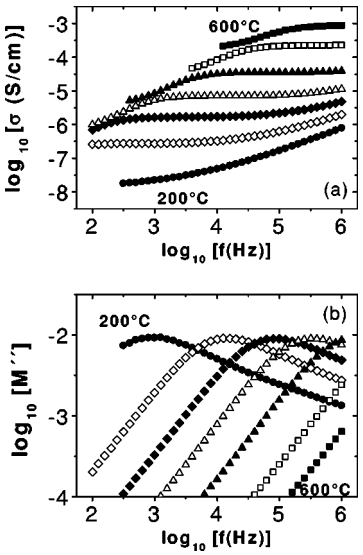

FIG. 1. Electrical relaxation measurements of $Gd_2Ti_{0.2}Zr_{1.8}O_7$. (a) Frequency dependence of the real part of the conductivity, at several temperatures [600 (■), 500 (□), 400 (▲), 339 (△), 300 (◆), 247 (◇), 200 °C (●)]. (b) Frequency dependence of the imaginary part of the electric modulus at the same temperatures shown in (a).

$$\sigma^*(\omega) = \sigma_{dc}[1 + (j\omega/\omega_p)^m], \quad 0 \leqslant m < 1, \tag{1}$$

which is the sum of the dc conductivity σ_{dc} and a power law term with fractional exponent m. The characteristic frequency ω_p marks the onset of the power law dependence $[\sigma'(\omega) \propto \omega^m]$, and it is thermally activated with the same activation energy E_{dc} of dc conductivity. The frequency dispersion of the ac conductivity is related to the hopping dynamics of mobile ions. dc conductivity can be obtained from plateau values at each temperature in Fig. 1(a).

Alternatively, in terms of the electric modulus, $M^*(\omega) = 1/\varepsilon^*(\omega) = j\omega\varepsilon_0/\sigma^*(\omega)$, the ion hopping ac conductivity can be expressed by the Fourier transform of the time derivative[13,15]

$$M^*(\omega) = \frac{1}{\varepsilon_\infty}\left[1 - \int_0^\infty \left(-\frac{d\Phi}{dt}\right)e^{-j\omega t}dt\right] \tag{2}$$

of a Kohlrausch[15,16] stretched exponential relaxation function of the form

$$\Phi(t) = \exp(-(t/\tau)^{1-n}), \quad 0 < (1-n) \leqslant 1. \tag{3}$$

In Eq. (2) ε_∞ is the permittivity at high frequencies. The characteristic relaxation time τ is approximately the inverse of ω_p in Eq. (1), $\tau \approx \omega_p^{-1}$, and it is therefore thermally activated with the activation energy of the dc conductivity. Figure 1(b) presents the frequency dependence of the imaginary part of the electric modulus for the same composition and temperatures. An asymmetric peak is observed at each temperature at a characteristic frequency $\omega_p \approx \tau^{-1}$, and good fits are obtained to Eqs. (2) and (3) from which the values of the exponent $(1-n)$ are obtained and observed to be temperature independent for each sample. The value of the high frequency permittivity, $\varepsilon_\infty = 35 \pm 6$, is found also to be almost independent of temperature and of Zr content in the whole series.

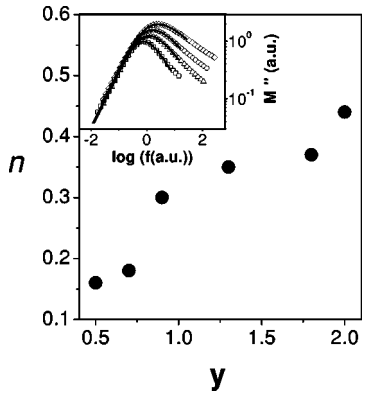

FIG. 2. Dependence of the exponent n, obtained from fits of electrical relaxation data to Eqs. (2) and (3) in the text, as a function of Zr content in $Gd_2Ti_{2-y}Zr_yO_7$. The inset shows the imaginary part of the electric modulus for samples with $y=2$ (◇), 1.3 (○), 0.9 (△), and 0.5 (□). Note that experimental data in the inset have been horizontally and vertically shifted for clarity.

Different models have been proposed to analyze electrical relaxation data in ionic conductors,[17,18] where fractional exponents m and n appearing in Eqs. (1)–(3) characterize ion hopping dynamics and are often related to the existence of cooperative effects among mobile ions. The coupling model[18–20] (CM) starts with the consideration of the independent hops of ions to vacant adjacent sites with exponential correlation function, $\Phi(t) = \exp(-t/\tau_o)$, and relaxation time τ_0. Such independent hops cannot occur for all ions at the same time because of ion-ion interactions and correlations. The result of ion-ion interactions is the slowing down of the relaxation rate at times longer than t_c of the order of 2 ps, changing the correlation function from $\exp(-t/\tau_0)$ to the Kohlrausch function in Eq. (3), wherein the fraction n is a measure of the cooperative effects. A major result from the CM is that the effective relaxation time τ is related to τ_0 by

$$\tau = [t_c^{-n}\tau_o]^{1/(1-n)}. \tag{4}$$

For ions vibrating in their cages and hopping to neighboring sites through barriers of energy E_a, the relaxation time for independent ion hopping is $\tau_o(T) = \tau_\infty \exp(E_a/kT)$. The reciprocal of τ_∞ is the attempt frequency of ions. It follows from Eq. (4) that the activation energy for the dc conductivity or τ will be larger than the energy barrier and given by the relation

$$E_{dc} = E_a/(1-n). \tag{5}$$

Increase of ion-ion interaction leads to higher degree of cooperativity in the ion hopping process, which corresponds to a higher value of n and consequently a higher activation energy for long-range ionic transport.

The inset of Fig. 2 presents the imaginary part of the electric modulus for samples with different Zr contents and shows how the peak broadens when Zr content is increased, corresponding to higher n values in the Kohlrausch function fit [Eq. (3)] to electric modulus spectra. The main part of Fig.

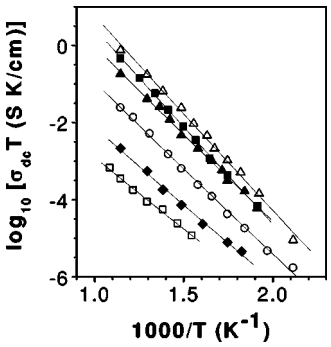

FIG. 3. Arrhenius plot of dc conductivity in the series $Gd_2Ti_{2-y}Zr_yO_7$ for different Zr contents [y=0.5 (□), 0.7 (♦), 0.9 (○), 1.3 (▲), 1.8 (△), and 2 (■)].

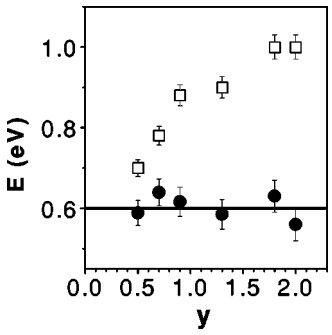

FIG. 4. Activation energies E_{dc} (□) and $E_a=(1-n)\ E_{dc}$ (●) as a function of Zr content in $Gd_2Ti_{2-y}Zr_yO_7$. Solid line represents the average value $E_a=0.60$ eV obtained for the energy barrier for oxygen hopping.

2 shows the systematic and significant increase in n as Zr content is increased from $y=0.5$ to 2.0. It is known that increasing Zr content above $y\geqslant 0.5$ results in creating vacant $48f$ sites which are responsible for oxygen hopping motion.[11] Recent XPS results have shown that increasing Zr content involves higher disorder in both the cationic and anionic sublattices.[7] Higher charge carrier (oxygen vacancies at $48f$ sites) concentration enhances mutual interactions and the more disordered structure fosters correlations. The trend of increase of the coupling parameter n with ion concentration (Fig. 2) is in accord with the precept of the CM that the coupling parameter n increases with ion-ion interactions engendered by higher density of ions.

Figure 3 shows the temperature dependence of the dc conductivity in an Arrhenius plot for different compositions. Dc conductivity is thermally activated with activation energies E_{dc} in the range 0.7–1 eV. At this point the question remains why the dc conductivity activation energy E_{dc}, as observed in Fig. 3, increases systematically with Zr content above $y=0.5$. This is shown more explicitly in Fig. 4. Interestingly, a result in the coupling model,[18–20] Eq. (5), predicts that an increase in the coupling parameter n, obtained from fits to electrical relaxation data by Eqs. (2) and (3), leads to a corresponding increase of E_{dc}. According to the coupling model, E_a is the activation energy for independent ion hopping or the microscopic energy barrier for oxygen ions to hop into neighboring vacant sites. Since both n and E_{dc} have been obtained from experiment, we can calculate now the energy $E_a=(1-n)E_{dc}$, and get an estimate of the energy barrier for oxygen ions to jump from $48f$ to $48f$ sites in the structures. A value of $E_a=0.60\pm0.03$ eV is obtained. Interestingly, this value is in excellent agreement with recent calculations from molecular dynamics simulations[8,9] (0.57–0.64 eV) and from static lattice energy minimization simulations[10] (0.58 eV) for the energy barrier oxygen ions must overcome to hop from $48f$ to $48f$ sites. Moreover, while the dc conductivity activation energy increases systematically with Zr content, the energy barrier remains constant within experimental error, indicating that the difference between the observed E_{dc} and E_a is due to the increasing slowing down of the oxygen ion hopping dynamics with decreasing temperature by the many-ions cooperative dynamics. Naturally the degree of cooperativity in the dynamics of the oxygen ion is enhanced by increasing ion concentration, and explains the larger difference between E_{dc} and E_a. We would like to point out that the observed correlation between $(1-n)$ and E_{dc} might be affected in ionic glasses by other factors like the Coulomb interaction among mobile ions and their charge compensation centers.[21–23]

To conclude, we have obtained evidence for the importance of cooperative effects in oxygen hopping dynamics in the oxygen ion conductor $Gd_2(Ti_{2-y}Zr_y)O_7$. Increasing the concentration of mobile oxygen vacancies results in enhancement of cooperativity and consequently in higher activation energies for long-range ion transport. Therefore, besides the concentration of vacancies and the energy barrier for single ion hopping, cooperative oxygen ion dynamics are shown to be a key factor in determining ionic conductivity values. This result might illuminate the search of novel conductors with optimized properties.

Authors from CINVESTAV-IPN thank CONACYT for financial support. Authors from Universidad Complutense acknowledge financial support from MCYT. K.J.M. thanks CINVESTAV-IPN for financial support during her stay at Universidad Complutense.

[1] A. V. Chadwick, Nature (London) **408**, 925 (2000).
[2] B. C. H. Steele and A. Heinzel, Nature (London) **414**, 345 (2001).
[3] P. Lacorre, F. Goutenoire, O. Bohnke, R. Retoux, and Y. Laligant, Nature (London) **404**, 856 (2000).
[4] J. B. Goodenough, Nature (London) **404**, 821 (2000).
[5] P. K. Moon and H. L. Tuller, Solid State Ionics **28-30**, 470 (1988).
[6] H. L. Tuller, Solid State Ionics **52**, 135 (1992).
[7] J. Chen, J. Lian, L. M. Wang, R. C. Ewing, R. G. Wang, and W. Pan, Phys. Rev. Lett. **88**, 105901 (2002).
[8] P. J. Wilde and C. R. A. Catlow, Solid State Ionics **112**, 173

(1998).
[9] P. J. Wilde and C. R. A. Catlow, Solid State Ionics **112**, 185 (1998).
[10] M. Pirzada, R. W. Grimes, L. Minervini, J. F. Maguire, and K. E. Sickafus, Solid State Ionics **140**, 201 (2001).
[11] C. Heremans, B. J. Wuensch, J. K. Stalick, and E. Prince, J. Solid State Chem. **117**, 108 (1995).
[12] A. J. Burggraaf, T. Van Dijk, and M. J. Verkerk, Solid State Ionics **5**, 519 (1981).
[13] K. L. Ngai and C. León, Phys. Rev. B **60**, 9396 (1999).
[14] A. K. Jonscher, *Dielectric Relaxation in Solids* (Chelsea Dielectric, London, 1983).
[15] P. B. Macedo, C. T. Moynihan, and R. Bose, Phys. Chem. Glasses **13**, 171 (1972).
[16] R. Kohlrausch, Pogg Ann. Physik **12**, 393 (1847).
[17] K. Funke, J. Non-Cryst. Solids **172-174**, 1215 (1994).
[18] K. L. Ngai and K. Y. Tsang, Phys. Rev. E **60**, 4511 (1999).
[19] K. L. Ngai and C. León, Phys. Rev. B **66**, 064308 (2002).
[20] K. L. Ngai and C. León, J. Non-Cryst. Solids **315**, 214 (2003).
[21] K. L. Ngai, J. N. Mundy, H. Jain, G. Balzerjollenbeck, and O. Kanert, J. Non-Cryst. Solids **95-96**, 873 (1987).
[22] W. C. Huang and H. Jain, J. Non-Cryst. Solids **188**, 254 (1995).
[23] W. C. Huang and H. Jain, J. Non-Cryst. Solids **212**, 117 (1997).